

# Notes Concerning Square-Root-Impedance (SRI) Amplifications Underestimating Full-Resonance (FR) Amplifications for Gradient Models

David M. Boore

Boore (2013) (B13 hereafter) discussed the comparison of FR and SRI amplifications for layered constant-velocity models and for gradient models. For the former, the SRI amplification underestimated the FR amplification at all resonance peaks, but the SRI amplification equals or is close to the rms of the total response (peaks and troughs) at frequencies higher than the fundamental mode frequency. For the gradient models the SRI amplification was less than the FR amplifications amplification for almost all frequencies, the exception being for low frequencies where the FR amplifications are generally a few percent lower than the SRI amplifications, although both amplifications are close to unity. Examples from B13 are given in Figures 1, 2, and 3.

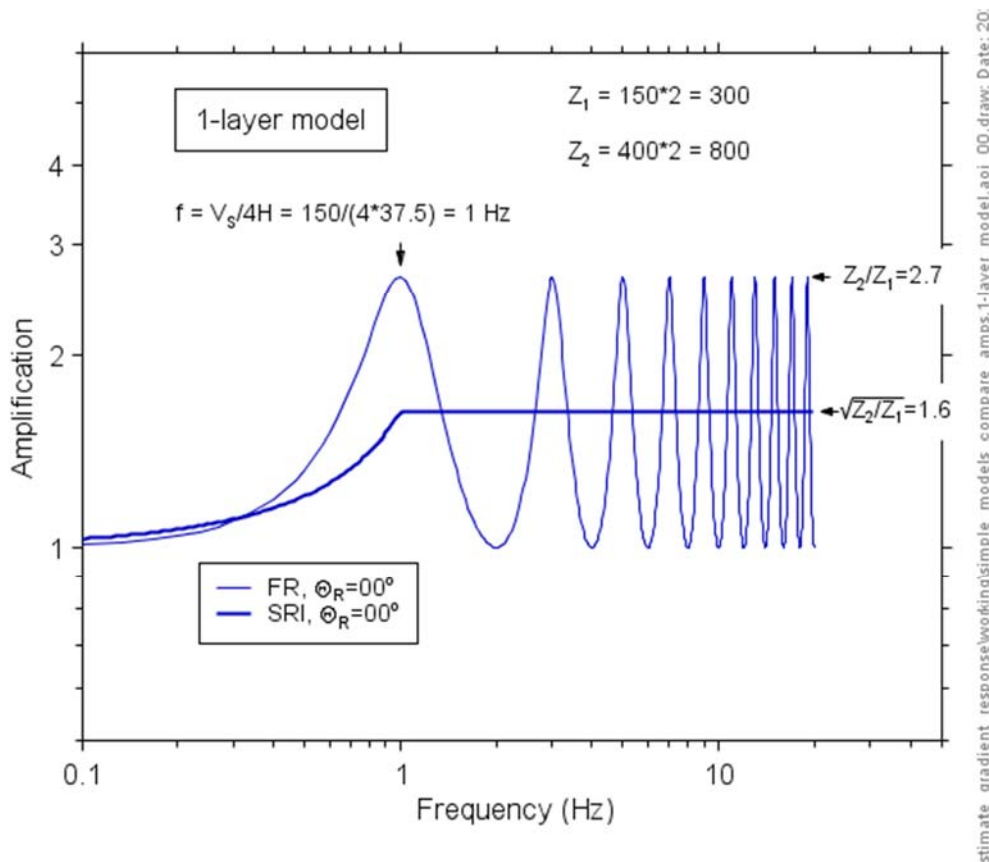
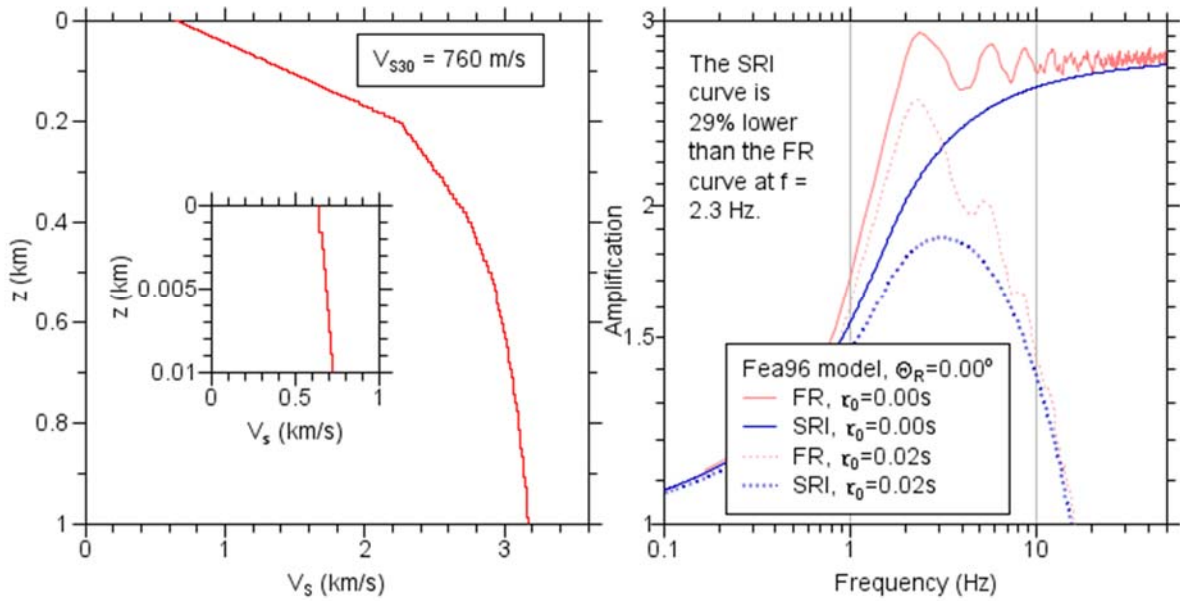
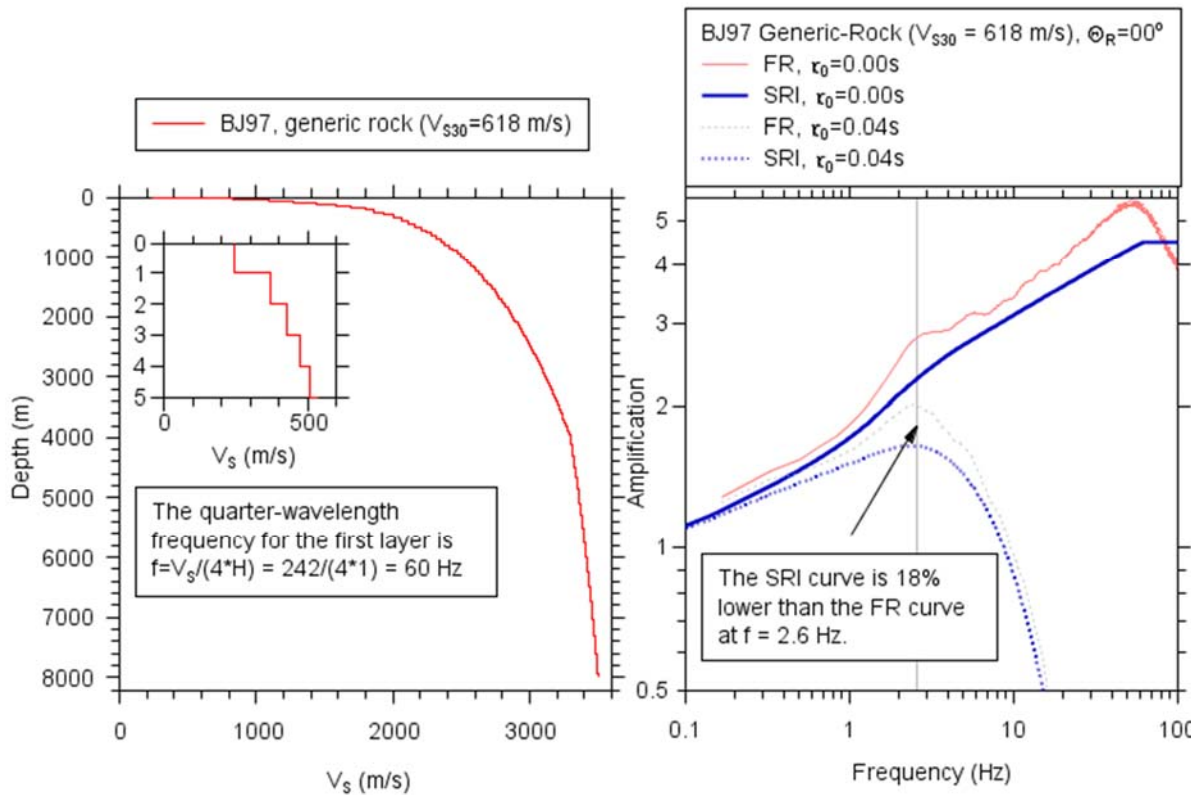


Figure 1. Revised from Figure 4 in B13.  $\theta_R$  is the angle of incidence.



File: C:\square-root-impedance\_site\_amps\sri\_nrrattle\_amps\gradient\_models

Figure 2. Reproduction of Figure 5 in B13.



File: C:\square-root-impedance\_site\_amps\sri\_nrrattle\_amps\gradient\_models\_for\_paj

Figure 3. Reproduction of Figure 6 in B13.

A reference was given in B13 to Poggi et al. (2011) who also found that the SRI response was less than the FR response for gradient models, as shown in their Figure 13. In addition, Scherbaum (2010) drew attention to the difference in his 23 December 2010 technical note prepared for the Pegasus Refinement Project [probably not easily available, so I should delete this and refer to Frank's 2011 email to me---if I can find it.] None of these articles speculated on the reasons for the differences. Such speculation is the purpose of these notes. On studying Figure 1, I was reminded that the peaks of the FR amplification are given by the ratio of seismic impedances (density times velocity) for this simple one-layer model, whereas the SRI amplification is given by the square-root of the ratio of seismic impedances. I think that this difference carries over to more complicated velocity profiles, where the FR amplifications can be thought of as being composed of the peak resonances for many layers. If correct, fundamentally the difference in FR and SRI amplifications is due to the FR amplifications being related to the ratio of seismic impedances in the model rather than to the square root of the seismic impedances, which is at the core of the SRI method. I have not, however, been able to find a way to verify this speculation theoretically or to use this insight to devise a procedure to adjust the SRI amplifications for gradient models so that they are consistent with the FR amplifications, short of replacing the SRI amplifications with FR amplifications. Instead, I will illustrate the differences between the FR and SRI amplifications for various models composed of a stack of constant-velocity layers (CVLs) that are equivalent to a gradient model. By "equivalent", I mean that the travel time from the surface to the bottom of any layer is the same as the travel time from the surface of the gradient model to the same depth as the bottom of a layer (see Boore, 2021, in the Data and Resources section for notes on obtaining equivalent velocity models).

### **The Velocity Models**

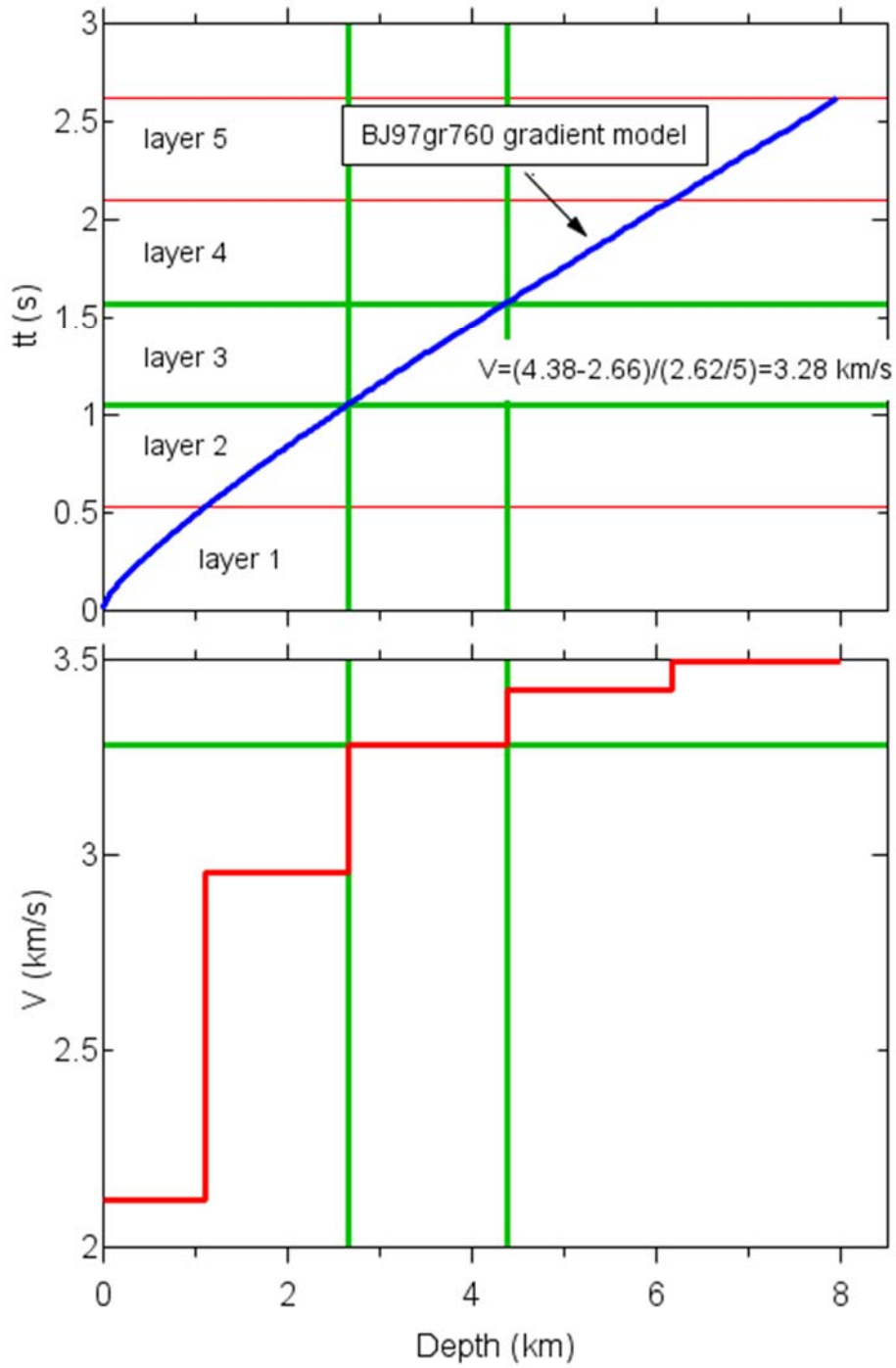
To obtain insight into the FR/SRI differences, in these notes I compute both types of amplifications for a series of models, based on the gradient model BJ97gr760 discussed in Boore (2016). That model is made up of lines connecting 273 velocity-depth points with no discontinuities except for a single 1-m thick CVL at the surface. The SRI amplifications are computed using *site\_amp\_batch*, which can use a velocity model made up of any sequence of CVLs or linear line segments connecting velocity-depth points. The FR amplifications, on the other hand, are computed using *nrrattle*, which requires a velocity model that is a stack of CVLs. The construction of the CVL model is discussed later.

As discussed above, it is my speculation the FR/SRI difference for gradient models might be because the FR amplifications can be thought as being composed of the peak resonances for many layers. Lacking an idea of how to assess this analytically, I rely instead on amplifications for a series of CVL models to illustrate how the FR amplifications are built up. I computed SRI and FR responses for a number of models with varying numbers of CVLs. In general, for a given number of layers the choice of layer depths and velocities are subject to two conditions: 1) the sum of the layer thickness must equal the thickness of the full model, and 2), the travel time

over the thickness of any CVL must equal the difference in the gradient model travel times from the surface to the depths bounding the CVL. Other than these constraints, the choice of the layer thicknesses is arbitrary. For the results here, I divided the surface-to-bottom of the BJ97gr760 model (8 km) travel time by the desired number of layers and found the depths corresponding to these travel times. I then computed the required velocity in each layer that satisfied constraint 2) above. For each layer I used the density-velocity relation in Boore (2016) to obtain the layer density. The procedure is illustrated in Figure 4, for one of the depths in a model with 5 CVLs. The essential ingredient in the procedure is the travel time vs depth. This was obtained from running *site\_amp\_batch* using the BJ97gr760 model. As shown in Figure 4, this travel time is divided evenly into 5 segments. The depth  $D$  for each segment is then extracted, from which all else follows.  $tt$  is the travel time from the surface to a depth  $D$ , and the velocity for layer  $i$  is given by

$$V_i = (D_i - D_{i-1})/\Delta tt$$

where  $\Delta tt$  is the difference in travel times from the surface to the bottoms of layers  $i$  and  $i - 1$ . As an aside, note that the quarter-wavelength frequency is given by  $f_{0.25\lambda} = 0.25/tt$ . The 5-layer CVL model is shown in the bottom graph of Figure 4.



File: C:\sri.underestimate\_gradient\_response\working\bj97gr760.tt\_and\_V\layer\_vs\_depth.draw; Date: 2021-09-08; Time: 17:55:52

Figure 4. Illustration of deriving the depths and velocities of a 5-layer CVL model.

Using the procedure just described, I constructed CVL models with 5, 10, 20, 40, 80, 160, and 320 layers. The velocity-depth plots for selected models are shown in Figure 5.

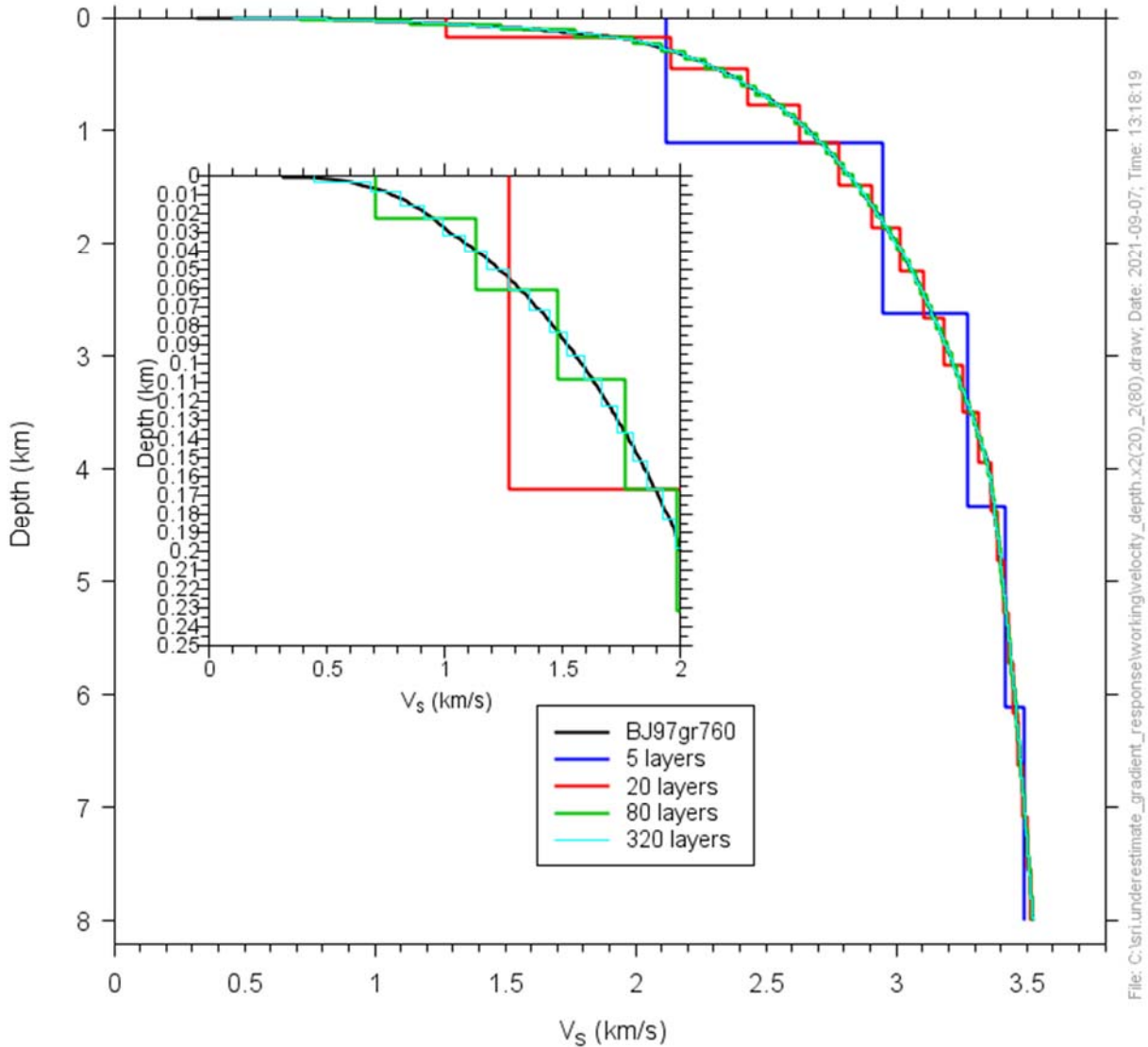


Figure 5. The velocity-depth profiles for a selection of the models considered in this note.

## Results

The FR and SRI amplifications are shown in Figure 6. The amplifications are relative to a halfspace with velocity = 3.5 km/s and density = 2.72 gm/cc. As noted earlier, the FR amplification calculations require a velocity model with CVLs, whereas the BJ97gr760 gradient model is composed almost entirely of non-constant-velocity layers. To resolve this apparent

inconsistency, I replaced the BJ97gr760 velocity model by models with equivalent CVLs comprised of 883 and 1200 layers. The FR amplifications for these two models are identical, reassuring me that the approximation of the gradient model by an equivalent CVL model with many layers gives an accurate representation of the amplifications for the gradient model.

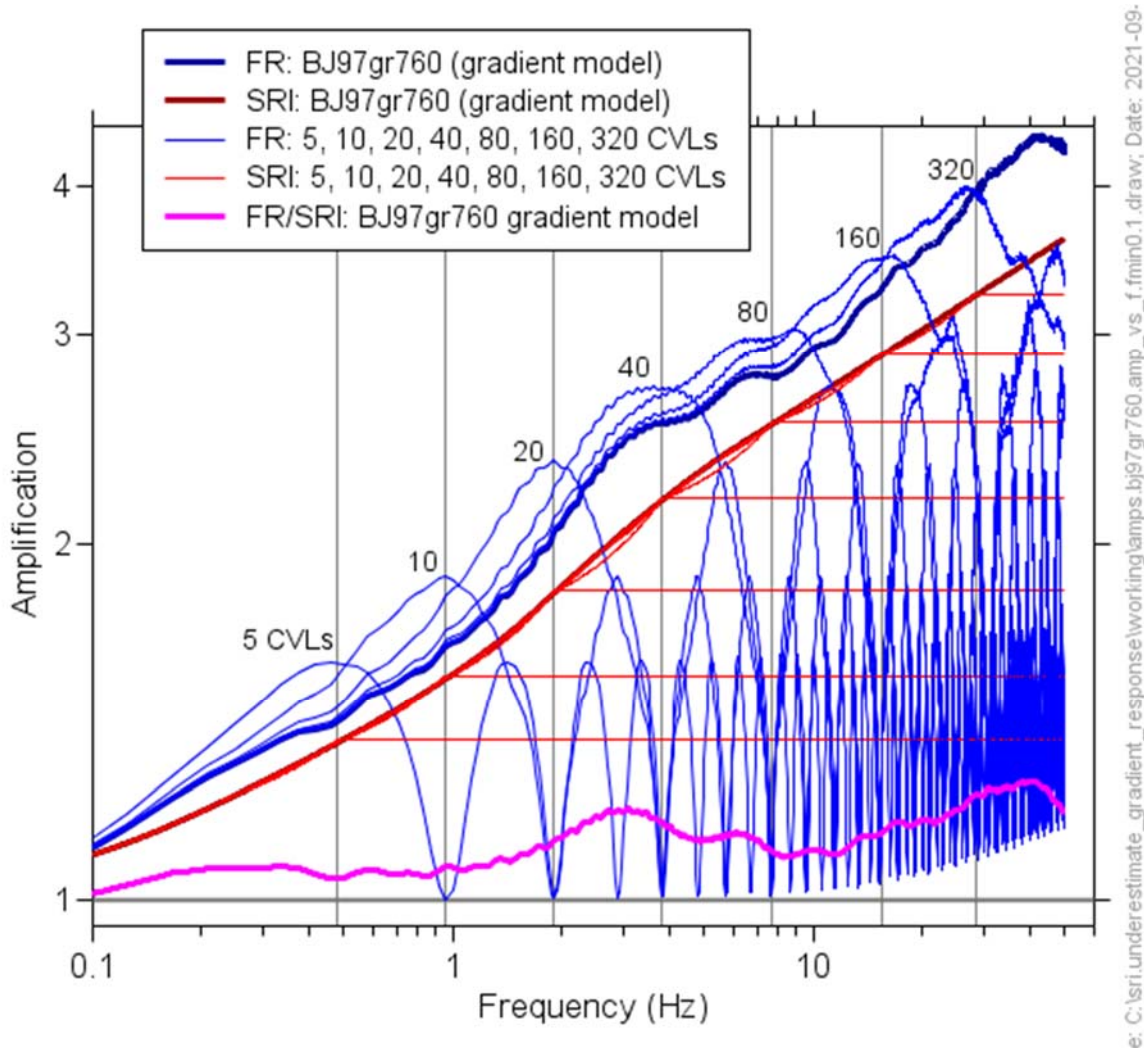


Figure 6. Amplifications for the various models. The number of layers in the CVL models is given by a number above the curve for that model; the vertical line to the right of the number is the resonant frequency for the uppermost layer in the CVL model.

There are two aspects of the results shown in Figure 6 that warrant discussion: the frequency of the first amplification maximum for each CVL model, and the amplitude of that maximum compared with the FR and SRI amplifications for the gradient model at that frequency. Some properties and results for the CVL models, of relevance for this discussion, are included in Table 1.

Table 1.

| Model <sup>‡</sup> | Layer#  | Thick (km) | V (km) | $\rho$ (gm/cc) | $f_{0.25\lambda}$ <sup>†</sup> (Hz) | $A_{FR:CLV}$ <sup>#</sup> | $A_{FR:gradient}$ <sup>#</sup> | Z2/Z1 | Zref/Z1 <sup>*</sup> |
|--------------------|---------|------------|--------|----------------|-------------------------------------|---------------------------|--------------------------------|-------|----------------------|
| 20 CVLs            | 1       | 0.167      | 1.275  | 2.24           | 1.91                                | 2.34                      | 2.03                           | 1.81  | 3.33                 |
|                    | 2       | 0.280      | 2.137  | 2.42           |                                     |                           |                                |       |                      |
|                    | 18 more | :          | :      | :              |                                     |                           |                                |       |                      |
| 80 CVLs            | 1       | 0.023      | 0.711  | 2.10           | 7.72                                | 2.97                      | 2.76                           | 1.68  | 6.38                 |
|                    | 2       | 0.038      | 1.138  | 2.21           |                                     |                           |                                |       |                      |
|                    | 78 more | :          | :      | :              |                                     |                           |                                |       |                      |

<sup>‡</sup>All models are underlain by a 3.5 km/s and 2.72 gm/cc halfspace

<sup>†</sup> quarter-wavelength frequency for first layer

<sup>#</sup> $A_{FR}$  is the amplitude of the FR model at the quarter-wavelength frequency, for the CVL and gradient models

<sup>\*</sup> $Z_{ref} = 3.5 * 2.72$  (halfspace velocity and density)

**Frequency of peak amplifications for CVL models:** The lowest frequency of the peak FR amplification for each CVL model corresponds to the quarter-wavelength frequency for the shallowest layer in each model. For example, the shallowest layer in the 20-layer model has a thickness of 0.167 km and a velocity of 1.275 km/s, giving a quarter-wavelength frequency of  $f_{0.25\lambda} = V/(4H) = 1.91$  Hz. Below this frequency the FR response of each CVL model follows the trend of the gradient-model FR amplification (and as expected, becomes closer to that amplification as the layers increase in the CVL models). Above the lowest frequency of the FR peak amplification, the CVL response resembles the response of a single-layer constant-velocity model, with a series of peaks and troughs. These observations are consistent with the FR response for a gradient model being built up of the fundamental mode resonant responses of many layers.

**Amplifications of CVL models:** The amplifications for the CVL models at the lowest peak frequency are always somewhat above the FR amplifications, with the CVL-model amplitudes approaching the gradient-model amplitudes as the number of layers increases, as expected. The FR amplifications are always greater than the SRI amplifications (for convenience, the ratio of FR to SRI amplitudes is included in Figure 6). Table 1 shows the amplifications based on ratios of the seismic impedances ( $Z = V\rho$ , where  $V$  and  $\rho$  are velocity and density, respectively), using two extremes for the reference impedance in the numerator: the impedance of the second layer in the model and the impedance of the halfspace. These predicted peak amplifications are formally correct for a layer over a halfspace, an assumption with decreasing validity as the number of layers increases. Despite this caveat, the CVL-model and gradient-model amplifications are between the predictions based on the ratio of seismic impedances and always above the SRI amplifications.



## Discussion

The frequencies of the amplification peaks for the CVL models and the comparison of the FR and SRI amplifications with those from the gradient models give some support to the speculation that the difference between FR and SRI amplifications for gradient models is because the former is controlled by the ratio of seismic impedances, whereas the latter is based on the square-root of the seismic impedance ratios. This implies that gradient models will always have FR amplifications greater than the SRI amplifications (as is well known to be true for the peak amplitudes of the fundamental mode resonances for models with strong impedance contrasts between layers). The differences in FR and SRI amplifications for gradient models is not large, however, and even though FR amplifications are easy to compute, there are advantages to using SRI amplifications. A number of these advantages are discussed in B13. An advantage not included in B13 is that the equations for computing the SRI amplifications allow for analytical equations to be used in inferring velocity profiles from ground-motion prediction models (Al Atik and Abrahamson, 2021).

## Data and Resources

No data were used in these notes. The amplifications used the following programs from the SiteAmp suite of Fortran programs: *site\_amp\_batch*, *f4nrattle*, *nrattle*, and *vel2constant\_velocity\_model*. The SiteAmp suite of programs can be downloaded from [http://www.daveboore.com/software\\_online.html](http://www.daveboore.com/software_online.html). Unpublished notes on constructing constant-velocity layered models are in Boore, D. M. (2021). *Constructing equivalent constant-velocity layered models*. 2021-10-26.pdf, available from [https://www.daveboore.com/daves\\_notes.html](https://www.daveboore.com/daves_notes.html). The figures were prepared using CoPlot ([www.cohort.com](http://www.cohort.com), last accessed November, 2021).

## Acknowledgments

I thank Linda Al Atik for drawing my attention to the differences in FR and SRI amplifications for gradient models and for reminding me that I had discussed this in my 2013 paper.

## References

Al Atik, L., and N. Abrahamson (2021). A methodology for the development of 1D reference  $V_S$  profiles compatible with ground-motion prediction equations: Application to NGA-West2 GMPEs, *Bull. Seismol. Soc. Am.* **111**, 1765–1783.

Boore, D.M. (2013). The uses and limitations of the square-root impedance method for computing site amplification, *Bull. Seismol. Soc. Am.* **103**, 2356–2368.

Boore, D. M. (2016). Determining generic velocity and density models for crustal amplification calculations, with an update of the Boore and Joyner (1997) generic site amplification for  $\bar{V}_s(Z) = 760$  m/s, *Bull. Seismol. Soc. Am.* **106**, 316–320.

Poggi, V., B. Edwards, and D. Fäh (2011). Derivation of a reference shear-wave velocity model from empirical site amplification, *Bull. Seismol. Soc. Am.* **101**, 258–274.

Scherbaum, F. (2010). On the applicability of the  $\lambda/4$  approximation to model the site amplification at the NPP sites, Pegasos Refinement Project TP2-TN-1135.